Investigation on Green Properties of Magnesium Alloy AZ31 Feedstocks Molded via Metal Injection Molding Process

Investigation on Green Properties of Magnesium Alloy AZ31 Feedstocks Molded via Metal Injection Molding Process

Nooraizedfiza Zainon[1*], **Mohd Afian Omar**[2], **Nur Liyana Mohd Rosli** [1], **Marina Marzuki** [1]

[1]School of Manufacturing Engineering, Universiti Malaysia Perlis, Kampus Tetap Pauh Putra, 02600 Arau, Perlis, Malaysia.
[2]Advance Materials Research Center (AMREC), SIRIM Bhd., Kulim Hi-Tech Park, Kedah, Malaysia.

*nooraizedfiza@unimap.edu.my

Abstract. Powder loading is an important parameter because of its role in part shrinkage, dimensional stability, and final density. Thus, this research investigated the properties of the molded magnesium feedstocks in determining the best powder loading for producing magnesium part through metal injection molding process. In this research, the feedstocks with three magnesium alloy AZ31 powder loading of (63, 65, 67) vol%, was prepared comprising the binder component of paraffin wax, high density polyethylene, waste plastic, and stearic acid (PW/HDPE/WP/SA) with weight fraction 55/21/14/10, respectively. After injection molding, the density, diamensional accuracy, and strength of the green part was investigated. The findings reveal that 65 vol% of powder loading resulting to the best green properties.

1. Introduction

The typical Metal Injection Molding (MIM) process comprises four stages which named mixing, injection molding, debinding and sintering. The mixture of powder and the binder system is called the feedstock which produced by the first step of MIM process. The feedstock is expected to be homogenous where each powder particles has been enveloped by a very thin film of binder and has a tight contact to each other. The feedstock desired to provide the rheological properties for injection molding [1-3]. The second stage in MIM is injection molding. The feedstock is injected into a desired shape by heating in the molding machine and forcing it under pressure into the tool cavity. This is accomplished by heating the feedstock to a temperature which allows it to flow. The temperature should be under the degradation temperature of the binder. Pressure is maintained on the feedstock during cooling in the mold to minimize the void formation [4-5]. Once sufficient cooling achieved, the green molding is ejected from the mold that has an adequate strength to be handled. Conventional plastic injection molding equipment is used to mold the feedstock into desired shapes. Although the flow behavior of MIM is quite similar to the plastic injection molding, typical MIM feedstocks flow less easily and freeze faster than the plastics. This is due to their high viscosity and high thermal conductivity which results in incomplete mold filling, especially in thin sections [6-8].

The solid loading is an important parameter in metal injection molding because of its role in part shrinkage, dimensional stability, and final density. Low solids loading causes part dimensional

variations during debinding and sintering, as well as product with low density. On the other hand, if the solid concentration is very high, the feedstock will be inhomogeneous and will not flow steadily in the injection molding machine generating dimensional inconsistencies in molded parts, with each pat having different dimensions [9-12]. In recent years there have been many investigations regarding powder loading of metal injection molding feedstock. Poh et al., [13] uses the thermogravimetric analysis and differential scanning calorimetry were used to determine the volume fraction of powder. The result reveals the highest powder loading was 46.96%. They also proved that TGA suitable for quantifying the point to point powder fraction in green compacts for ceramic materials as well as quality control of the feedstock. Aggarwal et al. [14] determined the optimal and critical solid loading based on simulation and rheological behavior (such as flowability, activation energy, and moldability index). Sotomayor et al. [15] studied on powder injection molding of premixed ferritic and austenitic stainless steel powders. They found that the optimum powder loading was established at 68 vol.%. Hidalgo et al. [16] reported the optimal loading of Invar 36 feedstocks resulted to be 57.5 vol.%. Schaper et al., [17] has successfully introduced AZ81 into the MIM process. However, the evaluation on green properties was not detailed discussed.

Thus, the aim of this study is to investigate the green properties of magnesium feedstocks henceforth the best feedstock formulation are determined. The density, dimensional accuracy, and green strength of the molded part have been studied.

2. Methodology

The Mg AZ31 feedstocks which containing certain fraction of metal powder, wetting agent, backbone polymer, and additives were developed to produce the green molded part. The magnesium powder with an average particle size of 22 μm supplied by MGH Industrial Co. Ltd, China with density of 1.734 g/cm^3 was used as a metal powder. The high density polyethylene (HDPE) with melting point of 134.5 °C which supplied by Titan Polyethylene (M) Sdn. Bhd, Johor Bharu and waste plastic (WP) with melting point 135 °C which supplied by SLT plastic Sdn. Bhd. Penang were used as a backbone polymer for the green molded parts with weight fraction of 21% and 14 %, respectively. Paraffin wax (PW) with a molecular weight of 380 g/mol and melting point of 59.4 °C used as a wetting agent. While, stearic acid (SA) with molecular weight 284.48 g/mol and melting point of 62.2 °C was used as a additives. Firstly, the feedstocks was prepared using Brabender at 160 °C at 50 rpm for 90 minutes. Three batches of the feedstocks were prepared with different powder/binder volume percentage which are (63/37), (65/35), and (67/33) as studied previously [18]. Then, the Mg feedstocks were molded on the vertical MCP 100KSA injection molding machine in tensile bar shape. According to [9] temperature used for the injection molding process was 140°C.

After injection molding, the green molded part were visually inspected to be free from any molding defect such as cracking, surface voids or distortion. The dimensions of the parts were measured and recorded. The recorded dimensions were very useful for further investigation, so that the changes in dimensions in subsequent processing could be followed. Each specimen was measured along its length and in three places, roughly equidistant from one another, across its thickness and width. The binder distributions in green mold parts were also examined on both the free and fracture surface using Hitachi TM3000 Tabletop Scanning Electron Microscope (SEM).

After injection molded, the molded part was then being measure for its density. The density of the molded part was then measured by applying Archemedes principles (ASTM B 962-14) [19] using electronic densimeter MD 300S. The densimeter machine provides a precision analytical balance which will permit readings within 0,01% of the test specimen and a beaker or vessel that is suitable for holding water of sufficient adaptability to immerse the specimens of various size. The test specimens may be supported in a wire basket. The samples were weighted in air and then in water. The density and the porosity of the molded part is given by Equation 1 and 2, respectively.

$$\rho_g = \frac{\rho_w W_a}{W_a W_b} \tag{1}$$

$$P_a = \left(\frac{W_c - W_a}{W_c - W_b} \right) \times 100 \quad (2)$$

where, ρ_w is a density of water, W_a is a weight of the sample on the air, W_b is a weight of the sample in water (g), and W_c is a weight after immersed in water.

The sample was then being measured for the green strength. The Autograph Shimadzu Precision Universal Tensile Machine used to perform the three point bending test (ASTM B 925-15) [20] on the molded part. 30 mm of support rollers with 50 mm span length used in the test and the peak load at fracture was recorded. The strength (S_g) of the green molded part was then calculated using Equation 3.

$$S_g = \frac{3PL}{2t^2 w} \quad (3)$$

Where P is a force required re to rupture, L is a length of the specimen span of fixture, t is a thickness of the sample, w is a width of the sample.

3. Results and discussions

Figure 1 shows the tensile shape of the injection molded parts (green molded parts) with a single gate which located at the end of the sample. At the beginning of the molding process, the molded parts facing several normal defects observed such as flow mark and powder/binder separation as shown in the Figure 2 (a) and (b), respectively. The flow mark may occurs due to insufficient heat on the Mg feedstock in the mold. Besides, the flow mark defects also may occurs due to the unstable flow at the flow front. Therefore, lowering injection speed and increasing the Mg feedstock temperature was done to troubleshoot this defect. Another defect observed was poor appearance around the gate which called powder/binder separation defect.

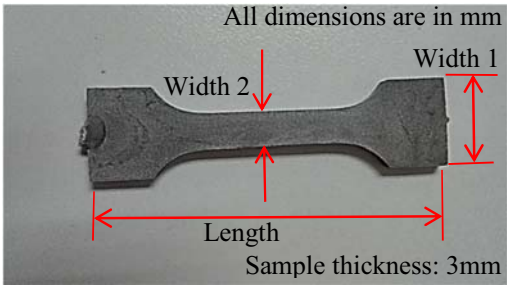

Figure 1. The dimensions of the green molded part.

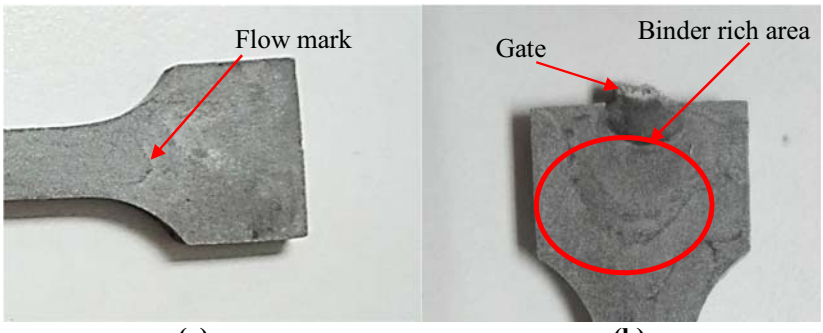

(a) **(b)**

Figure 2. The defects occurs on the molded parts (a) Flow mark (b) powder/binder seperation.

As the Mg feedstock passes through the narrow gate into the mold cavity, binder separation can occur due to powder migration from high shear rate region to a low shear rate region. The powder/binder separation become more serious at the end of filling stage and during the pressure holding stage wherein the Mg feedstock flows slowly and the pressure builds up rapidly. To fill in the clearance in the die cavity resulting from thermal shrinkage, more feedstock is pushed into these openings by the holding pressure. Since the movement of the metal powders in the feedstock is slow, due to the high interparticle friction, the binder which has low viscosity was forced to flow through interparticle intersections. Thus, the binder content at the gate areas is increased, causing the molding defects, particularly at the gate, where the shear rate is the highest. The separation will occur easily and form binder rich areas at the surface of the part near the gate.

According to [21] the gate redesign helps to alleviate this powder/binder separation problem. If the original gate has a narrow opening and is located at a thin section, it can be enlarged and relocated to a thick section. As a result. The level of powder/binder separation will be reduced and the flow marks will be minimized. However in this study, no redesign were made on the mold since thoroughly investigation are required on redesigning the mold which are out of the scope for this study.

3.1. Dimensional accuracy

The Mg feedstock with 67 vol% of powder loading exhibit the nearest values to the mold dimensions at all measured dimensions. Figure 3 shows the effect of powder loading on the percentage of molded shrinkage for Mg feedstocks containing 63, 65, and 67 vol% powder loading. The dimensions measured were length, which is parallel to melt flow, width perpendicular to the melt flow, and thickness which parallel to the mold opening direction. It expressed a decrease in dimensional variation as the powder loading increases. The increase of powder loading will produce greater number of point contacts between powder particles and restrict the movement of the particles. It is also translated into a smaller volume of binder and therefore smaller shrinkage occurred during solidification due to mold-melt interaction effect [22]. The percentage of the shrinkage measured also indicated that the shrinkage observed for the injected specimens are not uniform and was not according to the melted feedstock flow direction.

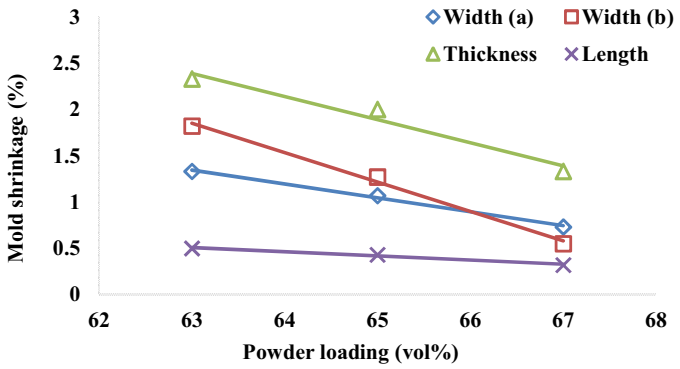

Figure 3. Shrinkage on the green molded parts at different dimensions for various powder loading.

3.2. Density of Molded Parts

Increasing the powder loadings result in greater packing density. The theoretical green density for (63, 65, and 67) vol% powder are summarized in Table 1. The densities are slightly lower than the theoretical which indicates the presence of a small fraction of voids in the molding. High green density of 67 vol% shows 1.79% reduction from the theoretical. Figure 4.55 shows the experimental and theoretical value for various powder loading. It shows that green molded parts with 63 vol% exhibits green density of 1.20-1.28 g/cm^3 while 65 vol% exhibits green density of 1.30 – 1.32 g/cm^3 and 67 vol% exhibits green density of 1.30-1.34 g/cm^3. The theoretical density for injected parts containing 63, 65, and 67 vol% are

1.31, 1.33, and 1.34 g/cm^3, respectively. Increasing the powder loading results in the greater packing density. The experimental density were slightly lower than the theoretical density which indicates the presence of small fraction of voids in the molding [23]. The parts containing 65 and 67 vol% powder loading both showing 98.70% of theoretical density as compared to 63 vol% which shows 94.98% of theoretical density. The better transmitted of molding pressure during injection, resulted in better packing of the Mg feedstock into the mold.

Table 1: The density, porosity and density reduction for the green molded parts.

Feedstock (vol%)	Theoretical density (g/cm^3)	Green density (g/cm^3)	Apparent porosity (%)	Percentage of density reduction (%)
63	1.3051	1.2396	5.1724	5.0190
65	1.3300	1.3122	0.0550	1.3380
67	1.3413	1.3234	1.2350	1.7900

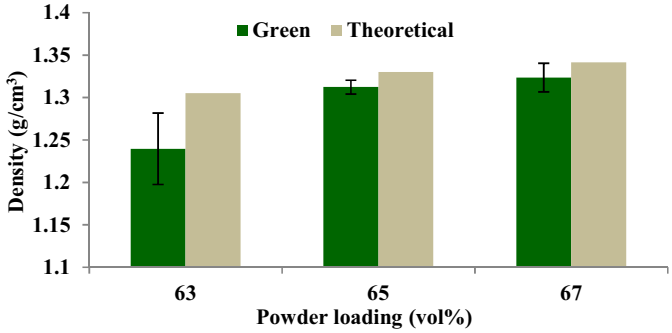

Figure 4: Graph of density of green molded parts for various powder loading.

3.3. Strength of Molded Parts

Table 2 shows the result of the 3 point bending test conducted on the green molded part to verify the strength provided by the binder content in the samples. The result reveals that the feedstock prepared with 37 vol.% of binder exhibits the highest strength after injection molded. The results proved that the binder plays an important role to strengthen the sample. The green strength decreased from 11.87 N/mm^2 to 6.13 N/mm^2 as the powder loading increased from 65 vol% to 67 vol%. The green strength decreased substantially with the increase of powder loading which translated into higher content of backbone polymer and therefore increase the strength of the green parts. This is because HDPE has the maximum strength as compared to the other components in the Mg feedstock. The increment of powder loading not only causes the percentage of backbone polymer (HDPE) decrease, but also decreases the forces between molecules by dispersing in HDPE molecule chains [8,24].

Table 2: The 3 point bending test results of molded parts with various powder loading.

Powder loading (vol%)	Maximum force (N)	Maximum Strength (N/mm^2)	Maximum Displacement (mm)	Maximum Strain (%)
63	7.8281	11.8358	0.6583	0.6077
65	5.5234	8.3512	0.5241	0.3711
67	4.0531	6.1282	0.2735	0.1936

4. Conclusions

For green molded part produce by magnesium feedstock, the densities for all formulation are slightly lower than the theoretical. The highest percentage of powder loading (67 vol.%) resulted to the highest density of molded parts which has only 1.79% of density reduction from the theoretical. However, the powder loading of 65 vol.% showing the lowest range of density measured for each samples which is indicated the best homogeneity among the feedstocks.

Acknowledgement

This research is supported by Fundamental Research Grant Scheme (FRGS) under a grant number FRGS/1/2016/TK03/UNIMAP/03/7 from Ministry of Education (MOE). Special thanks to Advanced Materials Process and Design Research Group, School of Manufacturing Engineering, UniMAP for the knowledgeable views during completing this research.

References

[1] Li, N., and Zheng, Y.: Novel magnesium alloys developed for biomedical application: A review. Journal of material science and technology **29**(6) (2013) 489-502

[2] Wolff, M., Schaper, J., Dahms, M., Ebel, T., Kainer, K. T.: Magnesium powder injection moulding for biomedical application. Powder metallurgy **57** (2014) 331-340

[3] Wolff, M., Schaper, J.G., Dahms, M., Ebel, T., Kainer, K.U., Klassen, T.: Magnesium powder injection moulding for biomedical application. In: Proceeding of the Euro powder metallurgy: Biomaterials, Salzburg, Brussels (2014)

[4] Santos, P., Niinomi, M., Liu, H., Cho, K., Nakai, M., Itoh, Y., Ikeda, M.: Fabrication of low-cost beta-type Ti-Mn alloys for biomedical applications by metal injection molding process and their mechanical properties. Journal of mechanical behavior of biomedical materials **59** (2016) 497-507

[5] Wolff, M., Schaper, J.G., Dahms, M., Ebel, T., Willumeit-Römer, R., and Klassen, T.: Metal injection molding (MIM) of Mg-alloys. In: Proceeding of 147th Annual Meeting and Exhibition, Volume 1., Pheonix, Switzerland (2018) 239–251

[6] Wolff, M., Schaper, J., Suckert, M., Dahms, M., F., F., Ebel, T., Klassen, T.: Metal injection molding (MIM) of magnesium and its alloys. Metals **6**(5) (2016) 118

[7] Wolff, M., Schaper, J., Sucket, M., Dhams, M., Ebel, T., Willumeit-Romer, R., Klassen, T.: Magnesium powder injection molding (MIM) of orthopedic implants for biomedical applications. The journal of the minerals, metals & materials society **68** (2016) 1191-1197

[8] Moballegh, L., Morshedian, J., Esfandeh, M.: Copper injection molding using a thermoplastic binder based on paraffin wax. Materials letters **59** (2005) 2832-2837

[9] Nooraizedfiza, Z., Salmah, H., Omar, M.A.: The effect of shear rate and temperature on rheology properties of magneisum metal injection molding feedstock. International review of mechanical engineering **7**(7) (2013) 1378-1383

[10] Romero, A., Herranz, G.: Development of feedstocks based on steel matrix composites for metal injection molding. Powder technology **308** (2017) 472-478

[11] Shivashankar, T., Enneti, R., Park, S. G., Atre, S.: The effects of material attributes on powder-binder separation phenomena in powder injection molding. Powder Technology **243** (2013) 79-84

[12] Haghshenas, M.: Mechanical characteristics of biodegredable magnesium matrix composites: A review. Journal of magnesium and alloys, **5** (2017) 189-201

[13] Poh, L., Della, C., Ying, S., Goh, S., Li, Y.: Powder distribution on powder injection moulding of ceramic green compacts using thermogravimetric analysis and differential scanning calorimetry. Powder technology **328** (2018) 256-263

[14] Aggarwal, G., Smid, I., Park, S. J., Randall, M. G.: Development of niobium powder injection molding Part II: Debinding and sintering. Refractory metals and hard materials **25** (2007) 226-236

[15] Sotomayor, M., Levenfeld, B., Varez, A.: Powder injection molding of premixed ferritic and austenitic stainless steel powders. Materials science and engineering A **528** (2011) 3480-3488
[16] Hidalgo, J., Morales, A. J., Barriere, T., Gelin, J. C., Torralba, J. M.: Water soluble Invar 36 feedstock development for μPIM. Journal of materials processing technology **214** (2014) 436-444
[17] Schaper, J.G., Wolff, M., Wiese, B., Ebel, T., Regine W.R.: Powder metal injection moulding and heat treatment of AZ81 Mg alloy. Journal of materiasl processing technology **267** (2019) 241-246
[18] Nooraizedfiza, Z., Omar, M.A., Rosliza, S., Marina, M.: Elucidating the influences of torque and energy in determining optimal loading. Materials today: proceedings **16** (2019) 2144–2152
[19] ASTM B962-14.: Standard test methods for density of compacted or sintered powder metallurgy products using Archimedes' Principle. In: ASTM International. West Conshohocken, PA (2014)
[20] ASTM B925-15.: Standard practices for production and preparation of powder metallurgy test specimens. In: ASTM International. West Conshohocken, PA (2015)
[21] Hwang, K.S. 2012 *Handbook of Metal Injection Molding*, ed D Heaney (Cambridge: Woodhead Publisher Limited) p. 109-131
[22] Hwang, K.S.: Common defects in metal injection molding (MIM). In: Handbook of Metal Injection Molding. (2012) 109-131
[23] Gershon, A.L., Gyger Jr., L.J., Bruck, H.A., Gupta, S.K.: Thermoplastic Polymer Shrinkage in Emerging Molding Processes. Experimental mechanics **48**(6) (2008) 789-798
[24] Raza, M., Faiz, A., Muhamad, N., Sulong, A., Omar, M., Akhtar, M., Aslam, M.: Effects of solid loading and cooling rate on the mechanical properties and corrosion behavior of powder injection molded 316L stainless steel. Powder Technology **289** (2016) 135-142.